



Strong Cube Texture Formation in Heavily Cold-Rolled Ni8W/Ni12W/Ni8W Composite Alloy Substrates Used in YBCO Coated Conductors

Yaotang Ji¹ · Hongli Suo¹ · Zili Zhang² · Lin Ma¹ · Jiazhi Li¹ · Chengxi Zhang¹ · Xingyu Wu¹ · Shaheen Kausar^{1,3} · Jin Cui¹ · Min Liu¹ · Yi Wang¹ · Qiuliang Wang²

Received: 16 September 2019 / Accepted: 27 October 2019 / Published online: 26 November 2019
© The Korean Institute of Metals and Materials 2019

Abstract

Three types of Ni8W/Ni12W/Ni8W composite substrates with strong cube texture, high yield strength, and low magnetization were produced by heavy cold rolling and annealing processes. The three types of composite substrates have the same thickness, but the ratios of thickness between Ni–8 at%W and Ni–12 at%W layer are different. The contents of tungsten exceed 9.3 at%, 10 at%, and 10.3 at% in the three types of obtained substrates. The presence of Ni alloys with higher W content in the Ni–12 at%W of the three composite substrates strongly enhanced the mechanical properties with about 290, 300 and 315 MPa respectively, and decreased the ferromagnetic behavior of the whole substrates. Additionally, it was found that an area that enhances cubic nucleation and growth in the Ni8W layer of composite substrates.

Keywords Multilayer structure · Texture · Strength · Magnetization

1 Introduction

Two routes, i.e. rolling-assisted biaxially textured substrate (RABiTS™) and ion beam assisted deposition (IBAD™) have been adopted to make 2G high-temperature superconductor tapes. The AMSC [1, 2] and BASF [3–5] are the two leading companies that use the RABiTS™ route, which can significantly reduce the price of the tapes. At present, the nickel alloy with 5 at% tungsten (Ni5W) is a widely used substrate for YBCO coated conductors (CC) [6, 7]. However, the Ni5W alloy substrate has ferromagnetic and low mechanical strength, which limits its application.

Due to their high yield strength and ease of forming cube texture, composite substrates with a tri-layer structure are a promising choice as substrate materials for coated conductors [8–13]. Sarma et al. [12] have reported the fabrication

of composite substrates by inserting a high-strength Ni12Cr alloy rod into a Ni–3 at% W tube, followed by hot rolling, cold rolling and finally annealing. Liu and Zhao [14–16] fabricated tri-layered different composite ingots Ni–5 at%W/Ni–12 at%W/Ni–5 at%W (Ni5W/Ni12W/Ni5W) and Ni–7 at%W/Ni–12 at%W/Ni–7 at%W (Ni7W/Ni12W/Ni7W) using the Spark Plasma Sintering (SPS) technique. Previously, a low W content was used in Ni–W composite substrates in the Ni–8 at%W layer because of the strong correlation of the texture developed during cold rolling and the stacking fault energy (SFE) of the metal or alloy. It was found difficult to obtain a sharp cube texture due to the decrease in SFE when the W content in Ni–W alloy exceeded 7% [17, 18]. Furthermore, alloying the Ni substrate with W decreases the Curie temperature of the substrates. To develop non-ferromagnetic substrates at the application temperature of 77 K, a W concentration of about 9.3 at% is necessary [19]. However, the Ni8W layer in the composite substrate with low W content can cause a higher magnetization and a lower mechanical strength in the substrate.

In our previous studies [20], we have prepared an ingot of the composition Ni–8 at%W/Ni–12 at%W/Ni–8 at%W (Ni8W/Ni12W/Ni8W), utilizing SPS (the W content of 9.3% excludes ferromagnetism at 77 K). Better results were obtained after additional intermediate annealing steps for optimizing the deformation process during cold rolling.

✉ Hongli Suo
honglisuo@bjut.edu.cn

¹ Key Laboratory of Advanced Functional Materials, Ministry of Education, College of Materials Science and Engineering, Beijing University of Technology, Beijing 100124, China

² Institute of Electrical Engineering, Chinese Academy of Sciences, Beijing 100190, China

³ Department of Physics, University of Peshawar, Peshawar 25120, Pakistan

Finally, the substrate with a strong cube texture had a lower Curie temperature and higher mechanical strength.

In this work, we change the ratio of the thickness of the Ni12W and Ni8W layers to enhance the total W content in the Ni8W/Ni12W/Ni8W ingots. The W content of three types of composite substrates became 9.3%, 10.0%, and 10.4%, respectively. As a result, we obtained composite substrates with lower Curie temperature, higher mechanical strength, and sharper cube texture. In this way, it was possible to overcome the limitations of SEF on obtaining sharp cube texture in the alloy substrates. So far, no other work is known on W contents as high as 10% while obtaining a strong cube texture in Ni–W alloy substrates.

2 Experimental

Alloys with the compositions Ni8W and Ni12W were mixed for a period of 6 h in a planetary ball mill using Ni (99.9%) and W (99.8%) powders under a protected atmospheric (Ar with 4 at% H₂). The mixed powders were packed into a graphite mold with the sequence Ni8W/Ni12W/Ni8W, followed by cold pressing under an axial pressure of 15 MPa. Three types of Ni8W/Ni12W/Ni8W composite ingots with the same overall thickness has different ratios (about 1:1, 1:2 and 1:3) of thickness between Ni8W layer and Ni12W layer. The cold-pressed composite ingots were sintered for five minutes at 800 °C under a pressure of 30 MPa (with the heating rate of 100 °C/min) by SPS technique. Then, the as-sintered ingot was given a homogenization annealing of 24 h at 1100 °C. The sintered ingots were then cold-rolled with thickness reduction from 8 mm to 100 μm at a reduced rate of about 5%. During the cold rolling process, four intermediate annealing steps (550 °C/120 min) were added at different rolling ratios at the thicknesses of (2, 1, 0.5, and 0.25) mm. After the thickness reached 100 μm, the cold rolled tapes were finally recrystallized by a two-step annealing process. The first step was performed at 700 °C/60 min, and the second step was performed at 1350 °C/120 min. All the heat treatment process was from room temperature, and the rate of temperature increase is 5 °C/min. Besides, the whole heat treatment process was performed in an Ar/4%H₂ atmosphere. The recrystallized texture of the composite substrates was characterized by scanning electron microscopy (SEM, QUANTA FEG 450) equipped with back-scattered electrons detector (EBSD, EDAX) and was evaluated by orientation image micrograph (OIM, TSL) software. The mechanical strength was tested using in situ tensile stage from TSL, which was adjusted upon the SEM stage for the EBSD analysis of dynamical deformation, while the

magnetic properties were measured using PPMS-14 from Quantum Design.

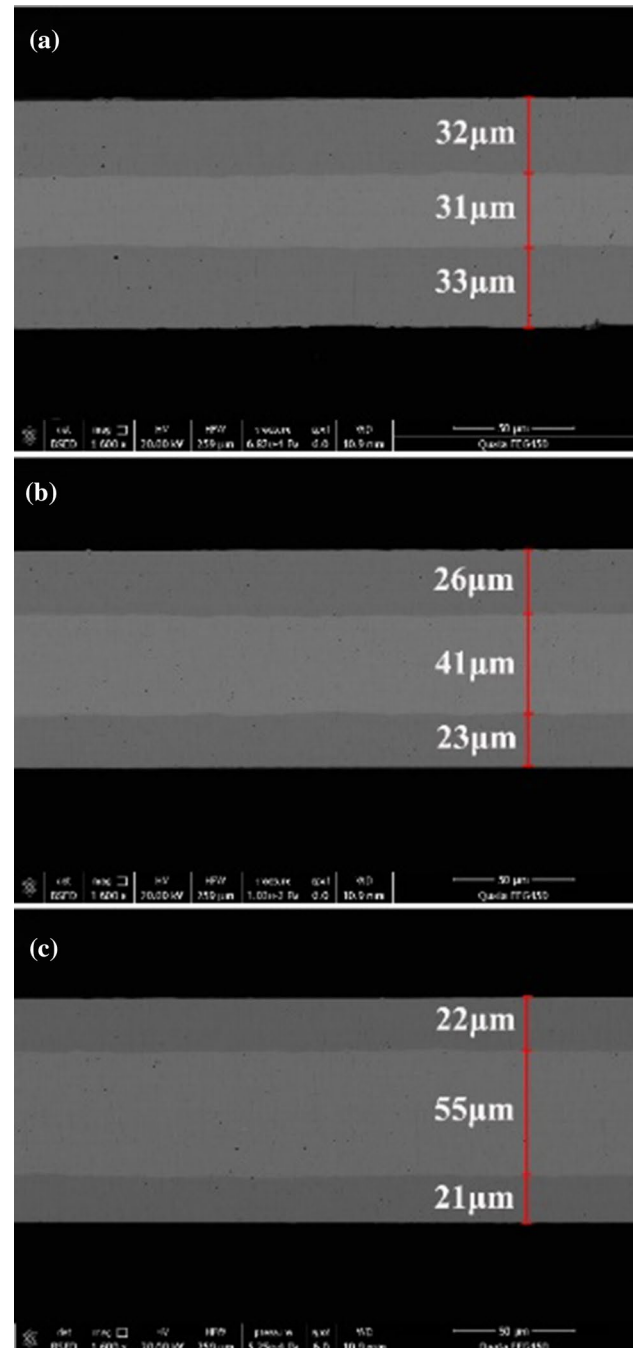


Fig. 1 SEM backscattering diffraction of **a** 111-, **b** 121-, and **c** 131-cold rolling composite substrates

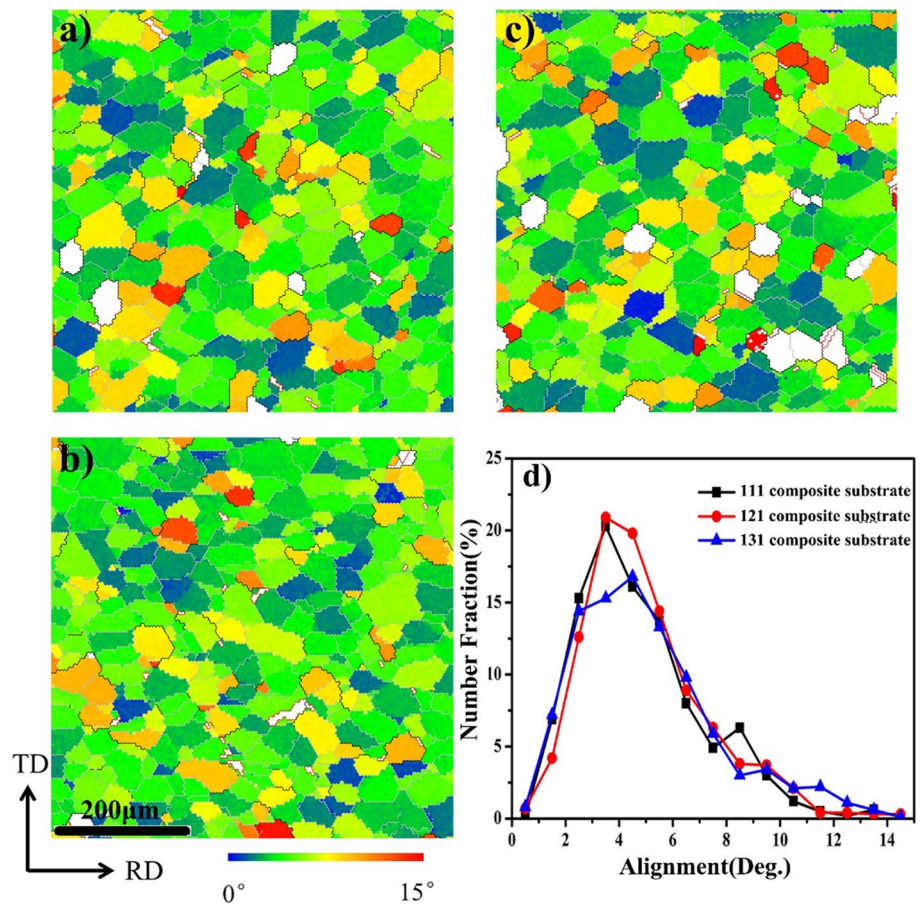
3 Results

The three types of obtained Ni8W/Ni12W/Ni8W composite substrates have different ratios (about 1:1, 1:2, and 1:3) of thickness between the Ni8W layer and Ni12W layer. Therefore, they are defined in the article as 111-, 121- and 131-composite substrates. Figure 1 shows backscattering images of the cross-section of 111-, 121- and 131-composite substrates after cold rolling. The sandwich structure of cold rolling composite substrates was observed. For all the three types of composite substrates which were subjected to high-temperature annealing, the large area of $600 \times 600 \mu\text{m}$ was randomly selected and analyzed by EBSD with a grid space of $5 \mu\text{m}$, to get local information of the orientation in the Ni8W layer of Ni8W. The fraction numbers of the cube texture alignment of the Ni8W surface layer for three different composite substrates were plotted in Fig. 2 (calculated by OIM). The percentages determined in the cube texture alignment of the three types of composite substrates were 94.7%, 95.6%, and 90.0% respectively, within a misorientation angle of 10° . The strong cube texture was observed in all the three types of composite substrates obtained by powder metallurgy and intermediate heat treatment during the

cold rolling process. Among the three types, the best cube texture content was found in the 121-composite substrate (1:2 thickness ratios between Ni8W and Ni12W layers). The texture evolution among the three composite substrates will be discussed later.

The ferromagnetism of the substrate causes AC losses in the practical application of coated conductors [21]. Figure 3a shows that the magnetization of three types of composite substrates and Ni5W substrates performed at 77 K of the operating temperature of coated conductors. It is observed from Fig. 3b that the saturation magnetization values of three types of composite substrates are 2.18, 1.34, and 0.76 emu/g, respectively. The magnetization values are significantly reduced by approximately 95% compared to that of Ni5W substrates. Figure 3c shows the magnetic change of Ni5W and three types of composite substrates within 5 K and 300 K in a magnetic field of 3500 Oe applied parallel to the substrate plane. The Curie temperature of the composite substrate is dramatically decreased contrast to the Ni5W substrate. Besides, the magnetic properties of 111-, 121-, and 131-composite substrates are sequentially lowered because the content of W was sequentially increased in the three samples. This result indicates that the use of the Ni8W

Fig. 2 EBSD data of composite substrates: misorientation distribution of the **a** 111-, **b** 121- and **c** 131-composite substrate, **d** cube texture content as a function of the deviation angle for different layer ratios



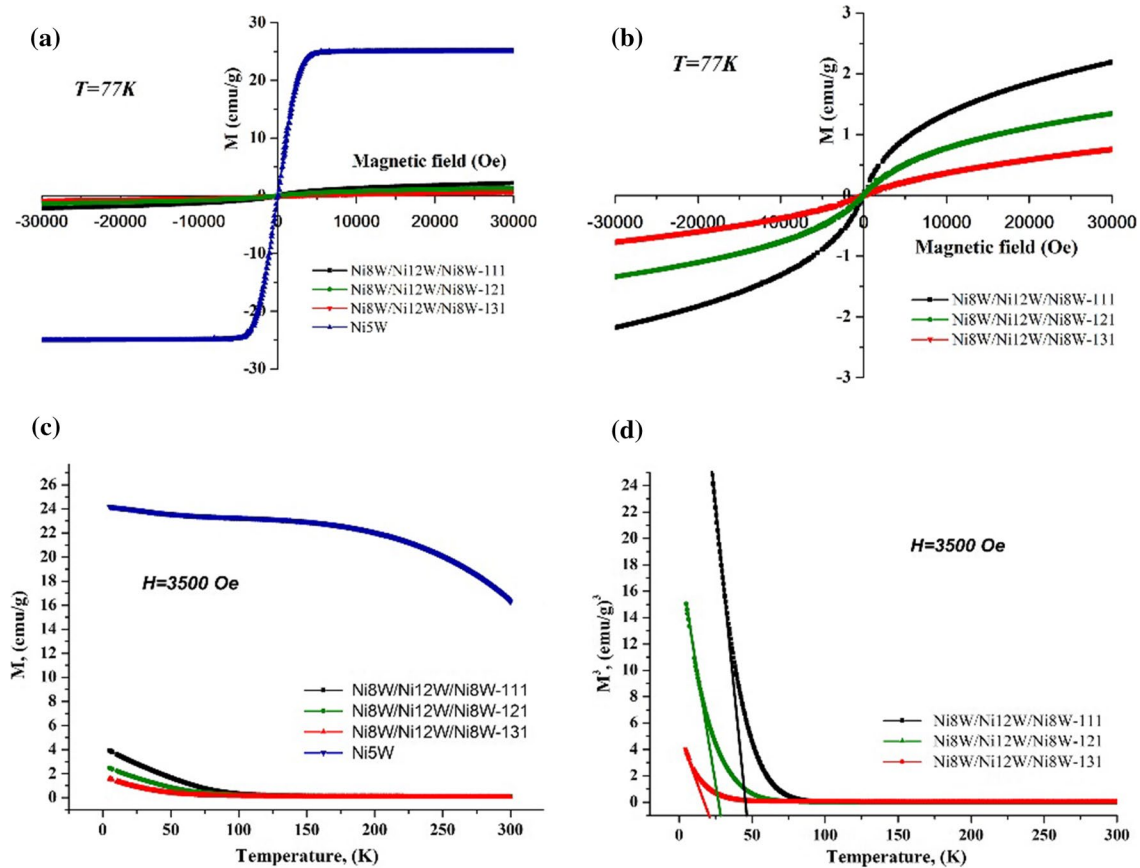


Fig. 3 a, b Magnetization loops at 77 K; c, d mass magnetization as a function of temperature for Ni5W and three types of composite substrates

and Ni12W layer in the composite structure significantly lower the magnetization of the whole substrate.

The composite substrates not only had a sharp cube texture and low ferromagnetism but also exhibited high mechanical strength. To evaluate their mechanical properties, the stress–strain test of the three types of composite substrates and Ni5W substrate were performed at room temperature, as shown in Fig. 4. It is found that through comparison the yield stress of the three types of composite substrates exceeds 290, 300, and 315 MPa, respectively, which is about 150 MPa larger than Ni5W substrates. Such high yield stress meets the practical application requirements of the coated tapes [22]. The higher yield stress results from the solid strengthening because of the high W content in the composite substrates.

4 Discussion

Figure 5 illustrates the locations of standard texture components of FCC metals in $\phi_2=0^\circ$, 45° , and 65° sections. From Fig. 6, it was found that the Ni8W layer surface of three different Ni8W/Ni12W/Ni8W composite substrates all formed

a cold-rolled texture dominated by S, Brass, Goss, and Copper texture after cold rolling. The texture type of 121- and 131- cold rolling composite substrate has almost the same texture type beside S, Brass, Goss, and Copper texture. The 121- and 131-composite substrates have some weak textures of other orientations apart from S, Brass, Goss, and Copper texture compared to 111-composite substrates. However, the most interesting result is that the 111- and 121-composite substrates formed a sharper cube texture, but 131-composite substrates did not after high-temperature annealing.

To further elaborate the dependence of the cold rolling texture of the Ni8W layer surface upon the formation of cube texture, the surface grain orientation was compared among the three types of composite substrates after heating at 700°C for 60 min (see Fig. 7). In the 111-composite substrate, it can be found that the cubic grains do not show the advantages of quantity and size. However, a higher content of the cubic grains is observed in the Ni8W layer of 121-composite substrates. Additionally, although the surface of the 131-composite substrate has the same cold rolling texture as the 121- composite substrates from XRD data, but the 131-composite substrates did not form as many cubic grains as 121-composite substrates after

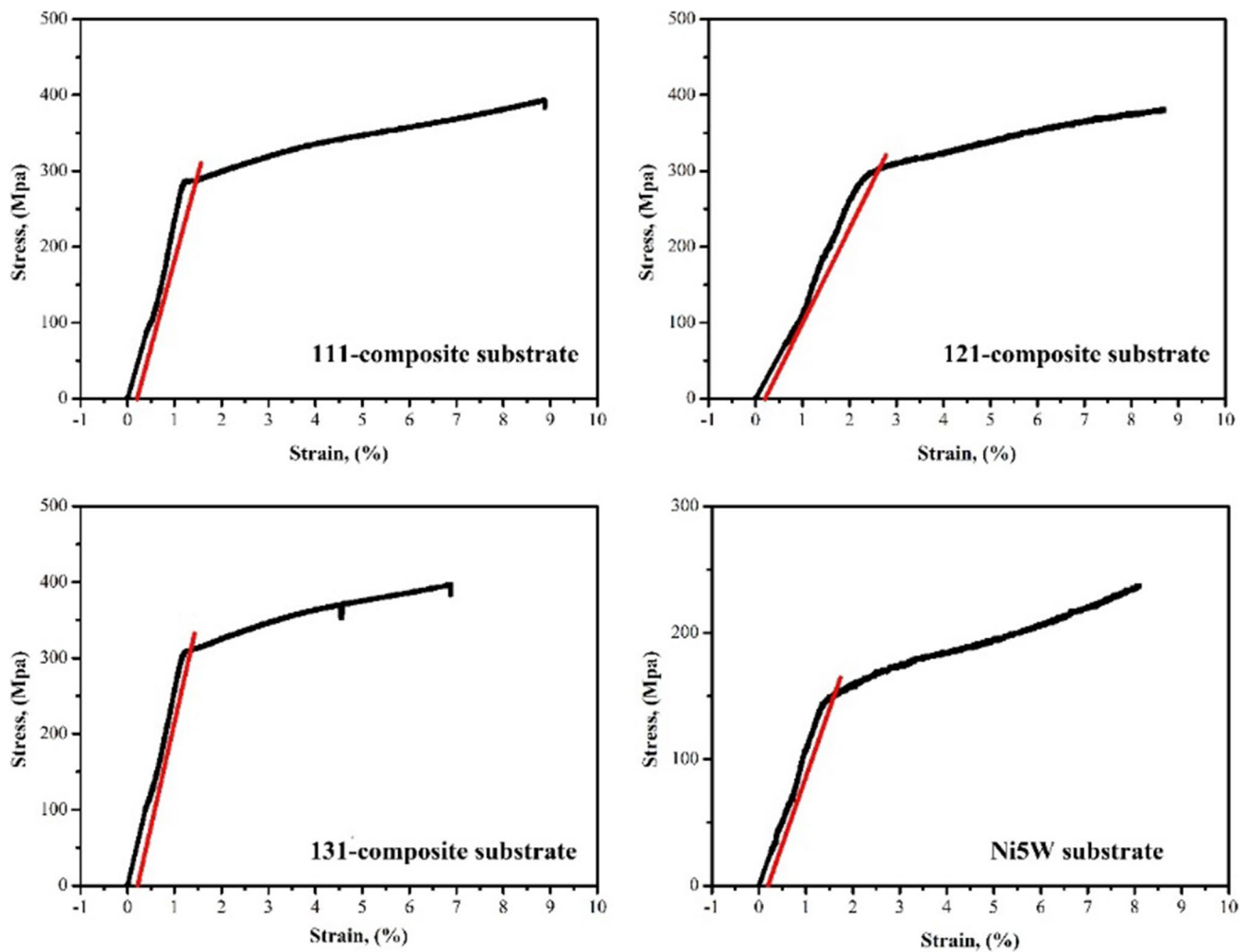
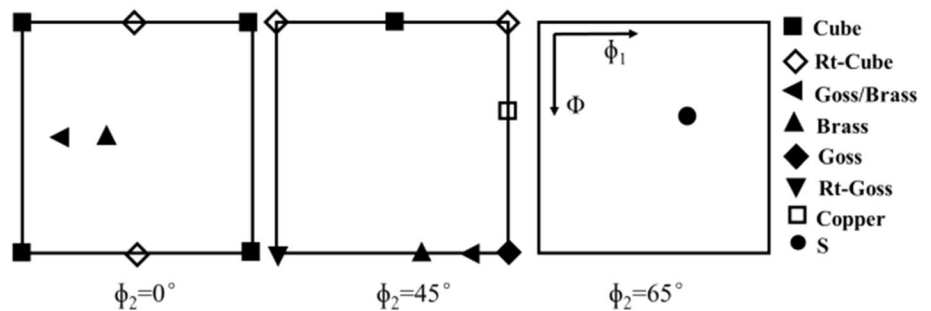


Fig. 4 Stress–strain curve of **a** 111-, **b** 121-, **c** 131-Ni8W/Ni12W/Ni8W substrate and **d** Ni5W substrate samples

Fig. 5 Locations of common texture components of FCC metals in $\phi_2 = 0^\circ$, 45° , and 65° sections



annealing. On the surfaces of 111-, 121-, and 131-composite substrates, 121- has the most recrystallized cubic grains followed by 111-composite substrates which have different cold rolling texture on the surface of Ni8W layer. This result indicated that the cold rolling texture of the surface in Ni8W layer does not play a decisive role in the formation of cube texture during the annealing process.

To learn the formation of the cube texture of composite substrates, the RD-ND cross-sections of the three composite substrates with different annealing are compared to the study. The quasi-in situ method [23–25] was used to demonstrate the same position of the different composite substrates at the different heating processes, respectively, as shown in Fig. 8. It can be found that the cubic grains marked by the

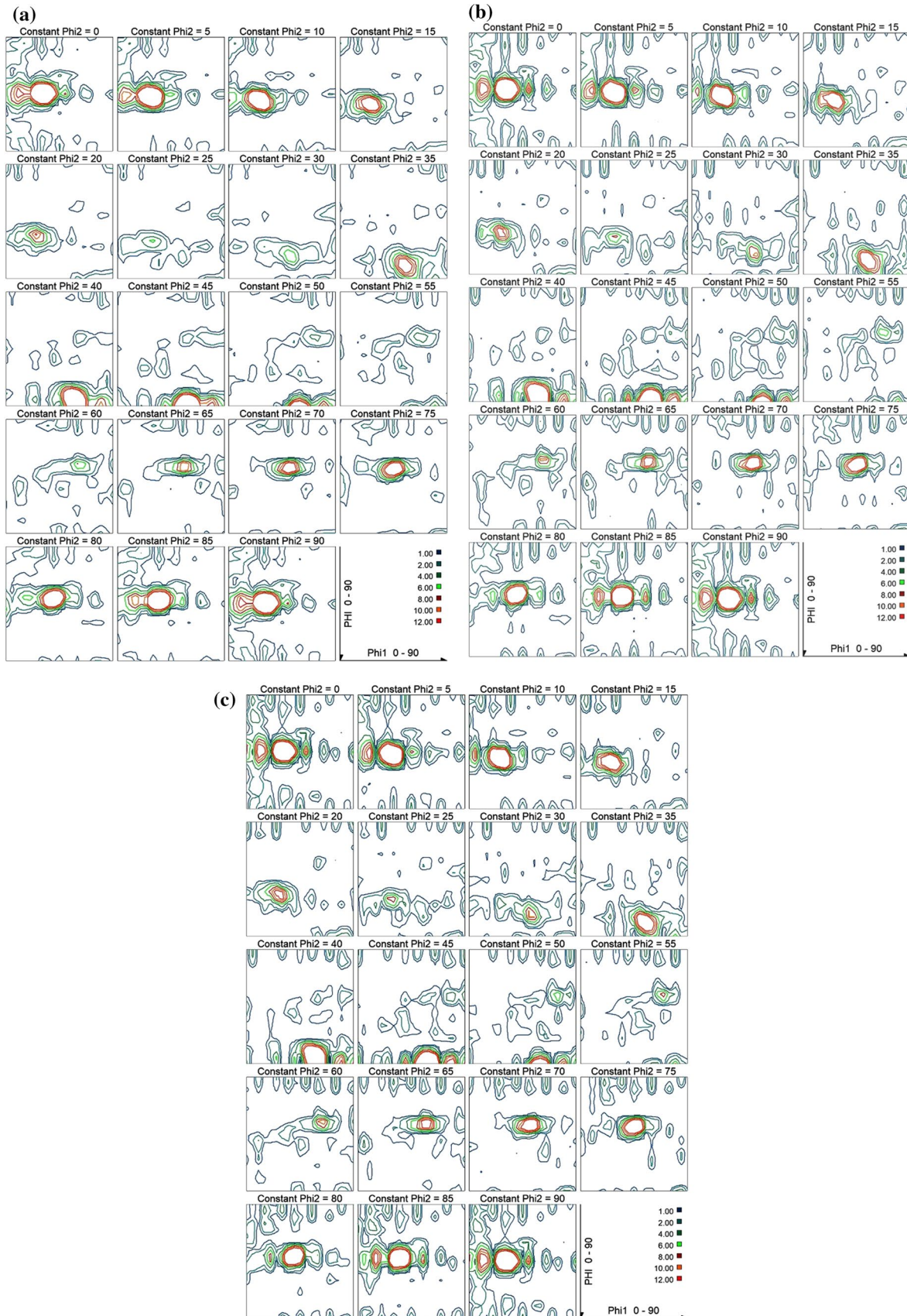


Fig. 6 ODFs for rolling textures of **a** 111-, **b** 121-, and **c** 131-Ni₈W/Ni₁₂W/Ni₈W substrate after cold rolling

Fig. 7 The IPF map of **a** 111-, **b** 121-, and **c** 131- composite substrates surface at 700 °C for 60 min

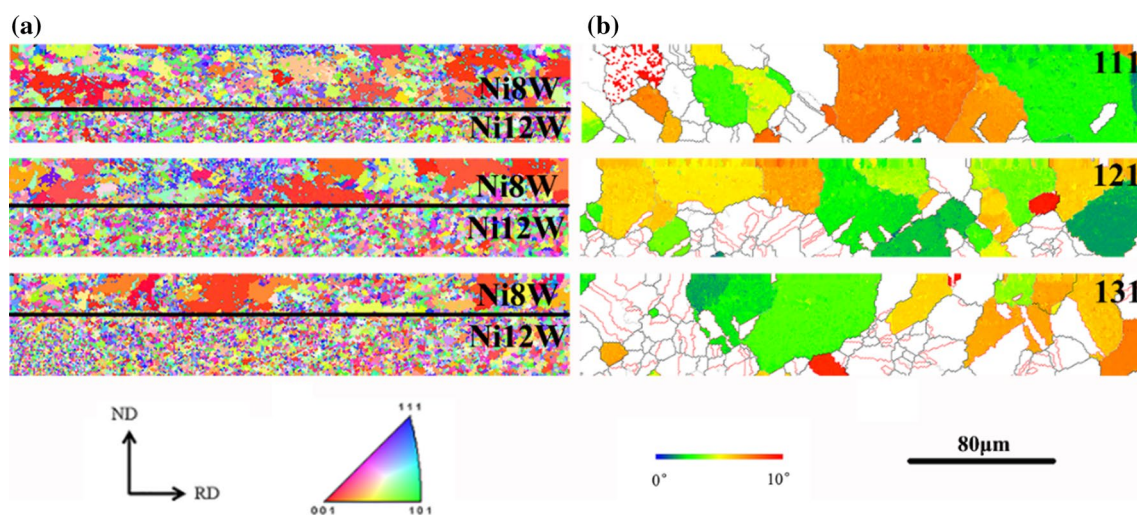
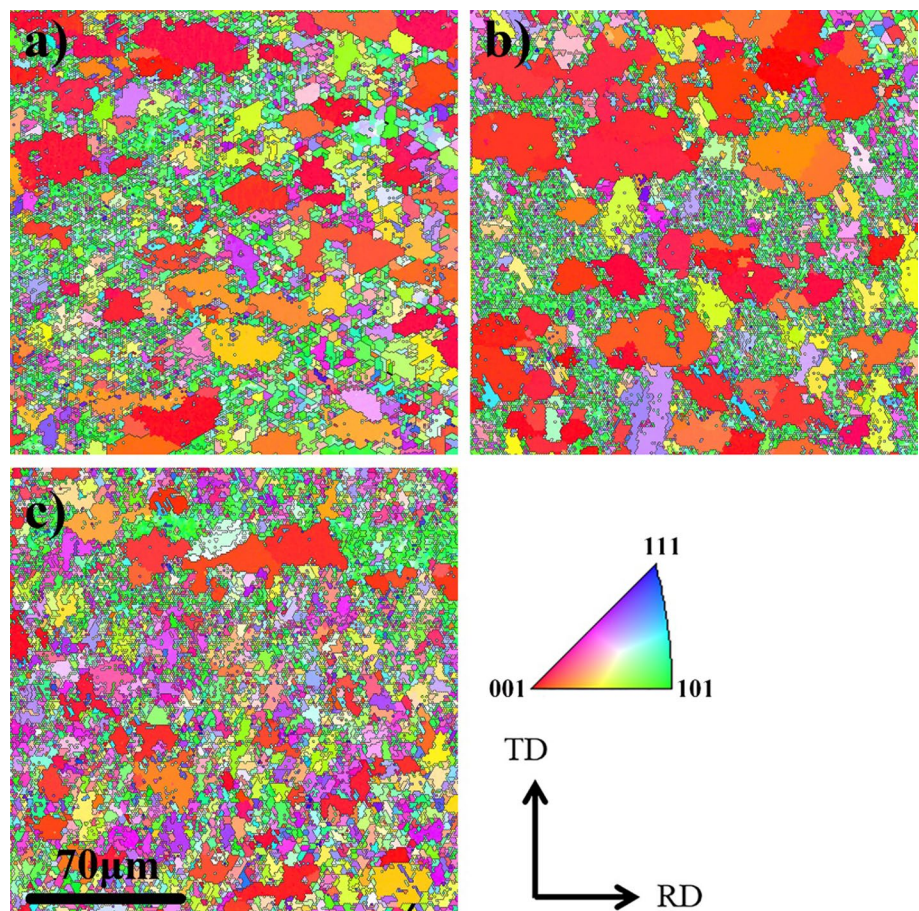


Fig. 8 **a** The IPF map of 111-, 121- and 131- composite substrates after 60 min at 700 °C, and **b** the EBSD map of the misorientation distribution in 111-, 121- and 131- composite substrates after annealing from 700 to 1300 °C

red color of the composite substrates mainly nucleated in the Ni8W layer and the grains of the Ni12W layer were gradually annexed by the grains of the Ni8W layer as the increase of temperatures. The three types of composite substrates all

formed a certain number of cubic grains after 60 min at 700 °C. The interesting thing is that the location and shape of cubic grains with red color in the three types of composite substrates are differently shown in Fig. 8a.

In the 121-composite substrates, the most recrystallized cubic grains are elongated in the RD direction and located at the Ni8W region which near the interface of Ni8W and Ni12W. In the 111-composite substrates, because the thickness of the Ni8W layer is bigger than the 121-composite substrates, the area of cubic grains does not dominate. Although there are also some cubic grains close to the interface of Ni8W and Ni12W, some other none-cubic grains with the same size as cubic grains in the outer region of these cubic grains. During the high-temperature annealing from 700 to 1300 °C, these none-cubic grains will grow up and limit the cubic grains to grow. In the Ni8W layer of 131-composite substrates, it can be found that the area of cubic grains is not less than 121-composite substrates, but these cubic grains do not have a long strip shape along RD direction. Because the three types of composite substrates have the same overall thickness and the formation of cube grains is mainly in the Ni8W layer, the thickness of the Ni8W layer has the greatest influence on the formation of cube texture.

Since the Ni8W layer in the 111-composite substrates is thicker than the 121-composite substrates, the outer part of the Ni8W layer is favorable for the nucleation of none-cubic grains. In this case, the none-cubic grains were not annexed by cubic grains during annealing. However, the thin Ni8W layer of 131-composite substrates was destroyed by the Ni12W layer during cold rolling. The recrystallized grains of these destroyed regions deviated cube orientation. Therefore, there is an optimum thickness of the Ni8W layer in the Ni8W/Ni12W/Ni8W composite substrate to facilitate the formation of cube texture.

To learn more about the nucleation of cubic grains at the interface of Ni8W and Ni12W, the RD-ND cross-section of the 121-composite substrates with the best cube texture after

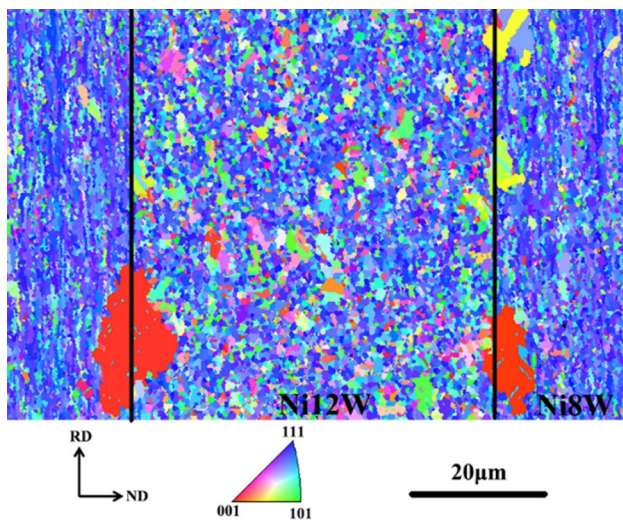


Fig. 9 The IPF map of 121-composite substrates at 700 °C holding 10 min

annealing was studied. Figure 9 represents the growth of the first nucleation region in the RD-ND section of the composite substrate after holding 10 min at 700 °C. It can be found that the region of cubic grains is in the Ni8W layer close to the Ni12W layer and the cubic grains has a long strip along the RD direction. This phenomenon also illustrates that there is an area in the Ni8W close to the interface that can be favorable for cubic grains to nucleate. The recrystallized grains are closely related to the rolling structure which can be reflected by the hardness of the sample. To evaluate the hardness of different positions of the RD-ND section, the Nano Indenter tested the hardness of the sample shown in Fig. 10. From the SEM image, it can be observed that the position 1, 2 and 3 are in the Ni12W layer, and position 4 and 5 are in the Ni8W layer. The hardness of positions 1, 2, and 3 are significantly higher than position 4 and 5 because of the difference of W content between Ni8W and Ni12W. The hardness of position 3 is slightly higher than 1 and 2 in the Ni12W layer, and position 4 is slightly higher than 5 in the Ni8W layer. Position 3 and 4 are all close to the interface, which explains the cold rolling structure close to the interface is different from the other position of the same layer. This result indicating that the region of Ni8W close to interface is good for nucleation of cubic grains.

5 Conclusion

Three types of Ni8W/Ni12W/Ni8W composite substrates with sharp cube texture, high yield strength, and low magnetization were prepared for coated conductors through the SPS technique. The W content in the three composite substrates were 9.3 at%, 10.0 at%, and 10.4 at% respectively. The three types of composite substrates have a high quality

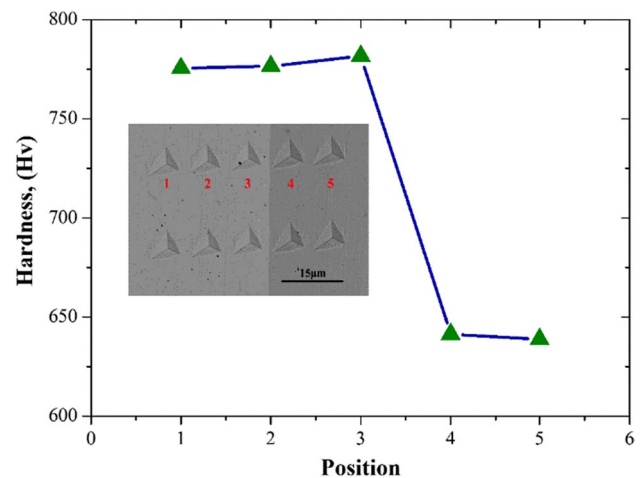


Fig. 10 The hardness of different positions at the 121-composite substrate section measured by nano indenter G200

of cube texture, of which the percentage was 94.7%, 95.6%, and 90.0% respectively within a misorientation angle of 10°. The high W content in the composite substrates not only enhanced the mechanical property but also decreased the magnetization at 77 K. The yield strength of the obtained 121-composite substrate with maximum content of cube texture exceeds 290 MPa while its saturation magnetization was substantially reduced by approximately 95% compared to that of Ni5W substrates. Besides, it was found that the thickness of the Ni8W layer plays a key role during the formation of cube texture. There is an area that is conducive to the formation of cubic texture close to the interface of the Ni8W layer and the Ni12W layer in the Ni8W layer. In conclusion, the successful manufacture of the three types of Ni8W/Ni12W/Ni8W composite substrates for YBCO coated conductors through the RABiTS process break the limitation of SFE on the formation of cube texture and provide an effective approach for manufacturing the super high tungsten Ni–W alloy substrates.

Acknowledgements This work is financially supported by the National Natural Science Foundation of China (51571002, 51777205, 11745005 and 51702316), by the General Program of Science and Technology Development Project of Beijing Municipal Education Commission of China (KM201810005010), by the Beijing Municipal Natural Science Foundation (2172008), by the Evaluation Research for the Performance of MgB₂ Tapes (GH-201809CG005) and by 211 Program of Beijing City and Beijing University of Technology, by the Program of Top Disciplines Construction in Beijing (PXM2019_014204_500031).

References

1. A.P. Malozemoff, *Phys. C* **530**, 65 (2016)
2. N.M. Strickland, S.C. Wimbush, M.W. Rupich, N.J. Long, *IEEE Trans. Appl. Supercond.* **29**, 1 (2019)
3. H. Rijckaert, G. Pollefeyt, M. Sieger, J. Hanisch, J. Bennewitz, K. De Keukeleere, J. De Roo, R. Huhne, M. Backer, P. Paturi, H. Huhtinen, M. Hemgesberg, I. Van Driessche, *Chem. Mater.* **29**, 6104 (2017)
4. H. Rijckaert, J. De Roo, M. Van Zele, S. Banerjee, H. Huhtinen, P. Paturi, J. Bennewitz, S.J.L. Billinge, M. Backer, K. De Buysser, I. Van Driessche, *Materials* **11**, 1 (2018)
5. M. Lao, P. Pahlke, M. Sieger, M. Falter, M. Backer, J. Hanisch, R. Huhne, M. Eisterer, *Supercond. Sci. Tech.* **32**, 1 (2019)
6. F. Gomory, M. Vojenciak, M. Solovyov, L. Frolek, J. Souc, E. Seiler, M. Bauer, M. Falter, *Supercond. Sci. Tech.* **30**, 1 (2017)
7. M.W. Rupich, X.P. Li, S. Sathyamurthy, C.L.H. Thieme, K. DeMoranville, J. Gannon, S. Fleshler, *IEEE. T. Appl. Supercond.* **23**, 6601205 (2013)
8. V.S. Sarma, J. Eickemeyer, A. Singh, L. Schultz, B. Holzapfel, *Acta Mater.* **51**, 4919 (2003)
9. H.L. Suo, Y. Zhao, M. Liu, L. Ma, *IEEE Trans Appl. Supercond.* **17**, 3420 (2007)
10. H.L. Suo, Y. Zhao, M. Liu, Y.X. Zhang, D. He, L. Ma, Y. Ji, M.L. Zhou, *Acta Mater.* **56**, 23 (2008)
11. H.L. Suo, M.M. Gao, Y. Zhao, Y.H. Zhu, *IEEE Trans Appl. Supercond.* **20**, 1569 (2010)
12. V.S. Sarma, B.D. Boer, J. Eickemeyer, B. Holzapfel, *Scrip. Mater.* **48**, 1167 (2003)
13. V.S. Sarma, B.D. Boer, J. Eickemeyer, B. Holzapfel, *Acta Mater.* **51**, 3769 (2003)
14. M. Liu, H.L. Suo, Y. Zhao, D. He, Y.X. Zhang, L. Ma, R.F. Fan, M.L. Zhou, *Scrip. Mater.* **56**, 129 (2007)
15. Y. Zhao, H.L. Suo, M. Liu, D. He, Y.X. Zhang, L. Ma, M.L. Zhou, *Acta Mater.* **55**, 2609 (2007)
16. Y. Zhao, H.L. Suo, Y.H. Zhu, M. Liu, D. He, S. Ye, L. Ma, R.F. Fan, Y. Ji, M.L. Zhou, *Supercond. Sci. Tech.* **21**, 72 (2008)
17. V.S. Sarma, J. Eickemeyer, L. Schultz, B. Holzapfel, *Scrip. Mater.* **50**, 953 (2004)
18. D.M. Liu, F. Hao, M.J. Li, Y.C. Hu, F. Gao, M.L. Zhou, *Mater. Sci. Tech.* **21**, 1387 (2005)
19. A.O. Ijaluola, J.R. Thompson, A. Goyal, C.L.H. Thieme, K. Marken, *Phys. C* **403**, 163 (2004)
20. D. Yu, H.L. Suo, J. Liu, L. Ma, J. Cui, Y.T. Ji, S. Kausar, M. Liu, Y. Wang, *J. Mater. Sci.* **53**, 15298 (2018)
21. H.R. Kerchner, D.P. Norton, A. Goyal, J.D. Budai, D.K. Christen, D.M. Kroeger, E.D. Specht, Q. He, M. Paranthaman, D.F. Lee, *Appl. Phys. Lett.* **71**, 2029 (1997)
22. A. Goyal, M.P. Paranthaman, U. Schoop, *MRS Bull.* **29**, 552 (2004)
23. L.X. Peng, X.W. Li, Z.J. Fan, C.L. Jiang, P. Zhou, X.C. Lai, *Mater. Charact.* **126**, 35 (2017)
24. X.C. Liu, Y.F. Sun, T. Nagira, K. Ushioda, H. Fujii, *J. Mater. Sci. Technol.* **35**, 1412 (2019)
25. H.L. Yang, S. Kano, L.J. Chai, J.J. Shen, Z.S. Zhao, J. McGrady, Z.G. Duan, H. Abe, *J. Alloys Compd.* **782**, 659 (2019)

Publisher's Note Springer Nature remains neutral with regard to jurisdictional claims in published maps and institutional affiliations.